

NUMERICAL PREDICTION AND HULL FORM REFINEMENT FOR SEAKEEPING IMPROVEMENT OF A CATAMARAN TYPE UNMANNED SURFACE VEHICLE

Muhammad Firdaus Aiman Mispua'ad^a, Nik Mohd Ridzuan Shaharuddin^{a,b*}, Mohd Hazmil Syahidy Abdol Azis^a

^aDepartment of Aeronautics, Automotive and Ocean Engineering, Faculty of Mechanical Engineering, Universiti Teknologi Malaysia, 81300 UTM Johor Bahru, Johor, Malaysia

^bMarine Technology Centre, Institute for Sustainable Transport, Universiti Teknologi Malaysia, 81300 UTM Johor Bahru, Johor, Malaysia

Article history

Received

12th August 2025

Revised

22nd October 2025

Accepted

4th November 2025

Published

2nd June 2026

*Corresponding email: nmridzuan@utm.my

ABSTRACT

The unmanned surface vehicle (USV) is specifically designed for targeted applications such as offshore environmental monitoring, hydrographic surveys and others. However, excessive motions in rough sea conditions can affect the accuracy of sensor data and may lead to potential equipment damage. Hence, this study aims to enhance the USV's seakeeping performance by improving the hull form design. The DELFT 372 model with a length between perpendiculars (L_{pp}) of 3.0 m and a hull separation of 0.46 m, was initially selected, modelled and validated before conducting seakeeping simulations using Ansys AQWA at a Froude number of 0.6. The simulated heave and pitch RAOs were then compared to published experimental results under Sea State 1 conditions for validation purposes. At $Fr = 0.6$ and a wave amplitude of 0.0179 m, the simulated heave and pitch RAOs were found to be 2.93 m/m and 94.25 °/m, with deviations of 4.61% and 8.96%, respectively compared to the published experimental data. The study then proceeds by slicing the original hull along its longitudinal centerline and repositioning the halves to form an outside-flat (OF) configuration, further modifying the bow to an X-bow design while maintaining the hull separation distance. The DELFT 372 OF-Xbow variant was also developed with an increased hull breadth from 0.12 m to 0.20 m. Seakeeping simulations were conducted for both modified configurations under Sea State 2 conditions at $Fr = 0.6$, where the wave amplitude is 0.25 m. The resulting heave and pitch RAOs were 0.97 and 0.96 respectively for the OF-Xbow at λ/L_{pp} of 9.69, and 0.90 and 2.09 for the OF-Xbow with 0.20 m demihull breadth, respectively. These values were compared to the symmetric hull, which exhibited heave and pitch RAOs of 0.80 and 2.67 respectively. The results indicate significant improvements in pitch motion of 64.17% for the OF-Xbow and 21.72% for the OF-Xbow with $b = 0.20$ m, compared to the symmetric hull. However, heave motion increased by 20.42% and 11.91% for OF-Xbow and OF-Xbow with $b = 0.20$ m respectively. This study demonstrates that hull modifications can effectively reduce pitch motion, although this comes at the cost of increased heave motion.

Keywords: Ansys AQWA, Asymmetry catamaran, DELFT 372 catamaran, Seakeeping Xbow

© 2026 Penerbit UTM Press. All rights reserved

1.0 INTRODUCTION

Traditionally, surveillance and monitoring activities performed using patrol boat with on-board human crews leading to substantial operational costs and safety concerns during rough sea conditions. Recently, USV technology finds increasing application in monitoring and surveillance activity. USV is fully equipped with electrical equipment and sensors according to the needs of operation such water quality monitoring. In order to get accurate data sample, all the sensors need to be on peak of its performance. Rough sea conditions can cause excessive motion, resulting in poor seakeeping performance and reduced accuracy of the collected data. According to Khan *et al.* [1], pH sensors are vulnerable to damage from excessive vibration and thermal shock. Therefore, these factors must be carefully addressed to ensure the USV functions efficiently and collects accurate data throughout its mission. According to Migeotte *et al.*, [2] one of the ways of vessel having better seakeeping performance is choosing catamaran hull type instead of monohull type. Figure 1 shows a USV developed by the authors at Universiti Teknologi Malaysia (UTM).



Figure 1: UTM-developed unmanned surface vehicle (USV)

In recent years, catamaran vessels have become one of the alternatives to substitute the contemporary monohulls. Catamarans generate less wave resistance than monohulls, while slender catamarans have lower added resistance in waves. In addition, catamaran ships have low resistance effect from the low draft compared to the monohull ship type [3]. Besides that, catamarans have a wide beam which increase the working area that contributes to transverse stability of the ship. According to Hadler *et al.*, [4], with the increase of stability of the vessel, it enhances the seakeeping characteristics of the vessel in moderate sea state. Despite having all these advantages, catamaran usage remains largely limited to regional trips over relatively short distances due to the typically narrow hull forms, which can result in seakeeping performance comparable to or even worse than that of monohulls [5-6]. Hence, performing seakeeping analysis especially heave and pitch motion characteristics and wave impact load is crucial in the initial stage of the catamaran design. Seakeeping performance of any vessel should be analyzed with respect to the sea state that the vessel required to operate [7].

Previously, seakeeping performance of ship analysis has been conducted by researchers using computational methods, in addition to theoretical and experimental methods. Strip theory methods have been applied in order to determine the seakeeping qualities of the catamaran theoretically [4]; [8-13]. Numerical study on the seakeeping characteristics of a high-speed multi-hull vessel in high sea states has been conducted by Castiglione *et al.*, [14]. Experimental models were tested on the seakeeping characteristics of wave-piercing catamaran in several of wave headings and wave height [15-17]. The effect of deadrise angle of deadrise angle variation along the hull length on seakeeping characteristics are evaluated experimentally by Begovic *et al.*, [18]. Fast catamaran in both regular and irregular waves has been studied by Bouscasse *et al.*, [19], Kim *et al.*, [20] and Diez *et al.*, [21] to assess the nonlinear effects into hull motion.

Numerical simulation has emerged as a reliable and accurate alternative to experimental methods, which are often costly, time-consuming and impractical for evaluating various seakeeping conditions of a catamaran. It can provide a simpler process for determining the hydrodynamic characteristics of any hull forms. The accuracy of the Computational Fluid Dynamics (CFD) results was validated through comparison with experimental data reported in studies [22–25]. Ozturk *et al.*, [26] has investigated a full-scale CFD study of resistance and seakeeping performance of a double-M boat constructed that comprises the benchmark DELFT 372 catamaran with an extra center and two side hulls. The estimation of the correct induced wave for analyzing seakeeping performance of a KRISO container ship has been conducted by Nguyen *et al.*, [27]. Fitriadhy *et al.*, [28] conducted an investigation by using CFD analysis on seakeeping performance of a training ship (full scale model) quantified through a RAO for heave and pitch motions. The effects of the application of the foil system on the seakeeping performance of vessels has been performed by Suastika *et al.*, [29]. Numerical prediction of ship motions especially heave and pitch of Wigley ship model heading over regular waves at Campos Basin, Brazil has been performed by Rocha *et al.*, [30]. Kiryanto *et al.*, [31] examined the design of hospital catamaran with good stability and seakeeping using a numerical method with the help of CFD using diffraction panel method.

Meanwhile, for asymmetrical catamarans, Sahoo *et al.*, [32] investigated the resistance characteristics of round bilge hulls and found that both total resistance and hull-to-hull interference increase as the clearance between the hulls decreases. Cirello *et al.*, [33] used experimental and computational methods to optimize asymmetrical catamaran hull shapes. Utama *et al.*, [34] examined the effects of lateral separation and longitudinal stagger on resistance at a Froude number of 0.7, concluding that certain hull configurations can reduce wave resistance at specific speeds. From Ikezoe *et al.*, [35], the OF type hull outperforms the “Inside Flat” IF type in terms of overall seakeeping performance, based on their experimental study on catamarans with asymmetrical demi-hulls.

Additionally, the X-Bow concept developed by the Ulstein Group aims to enhance a vessel's operability in rough sea conditions and unpredictable weather by minimizing vertical motions such as pitch and heave. Yehia *et al.*, [36] confirmed that beyond improving seakeeping performance, the Xbow design significantly reduces fuel usage, making vessels more energy-efficient. Their study on the energy efficiency of Xbow-equipped container ships concluded that the design yields substantial fuel savings at high Froude number. Basil *et al.* [37] conducted a study on the hull optimization of fishing trawlers using the Ulstein XBow and bilge keel designs. The results showed that the installation of bilge keels on Xbow Ulstein trawlers increased the roll period by at least 40% and reduced the roll amplitude by 15%. According to Chen *et al.* [38] at higher speeds ($Fr = 0.5$), the wave-piercing bow (XW1) shows smaller pitch motions than the X-Bow (XB1). At lower speeds ($Fr = 0.3$), XW1 produces larger motions in long waves. In general, XW1 gives greater motion responses for most wavelengths, but at large wave heights ($H = 0.12$), it can reduce heave motion, especially at higher speeds and longer waves ($\lambda/L > 1.8$). The research gap addressed in this study stems from the limited exploration of hull geometry modifications specifically aimed at reducing pitch motion, despite the critical influence of hull form on a vessel's seakeeping performance.

For unmanned surface vehicles (USVs), effective seakeeping is essential to ensure mission success, sensor accuracy and structural integrity. Pitch, being a dominant motion in longitudinal wave conditions can significantly impair these operational factors. Although minimizing pitch is vital for optimal USV performance, research focused on hull form variations designed to mitigate pitch remains scarce. This gap underscores the need for further investigation into how targeted modifications to hull geometry can improve pitch response and overall seakeeping behavior. To address this, the present study incorporates asymmetric demi-hulls featuring an outside flat surface combined with an Xbow design into the USV configuration. This design aims to enhance seakeeping performance during

ocean operations and enables the evaluation of its effectiveness under realistic service conditions by modifying the DELFT 372 into OF and OF-Xbow.

2.0 METHODOLOGY

2.1 DELFT 372 catamaran hull

The DELFT 372 catamaran hull is a widely used benchmark model, with extensive research conducted on its hydrodynamic performance. A substantial body of literature exists, encompassing resistance and seakeeping studies, both using towing tank experiments [19]; [39] and numerical simulations [14];[16];[26] involving this hull form. In the present study, Rhino 6 software is utilized to model the DELFT 372 catamaran hull. Prior to initiating the modelling process, several key parameters were defined for generating the lines plan. Figure 2 illustrates the lines plan used as a reference during the hull tracing process. The hydrostatics data of the basic model which is based on the DELFT 372 symmetry will be verified against the benchmark DELFT 372 by Veer [39].

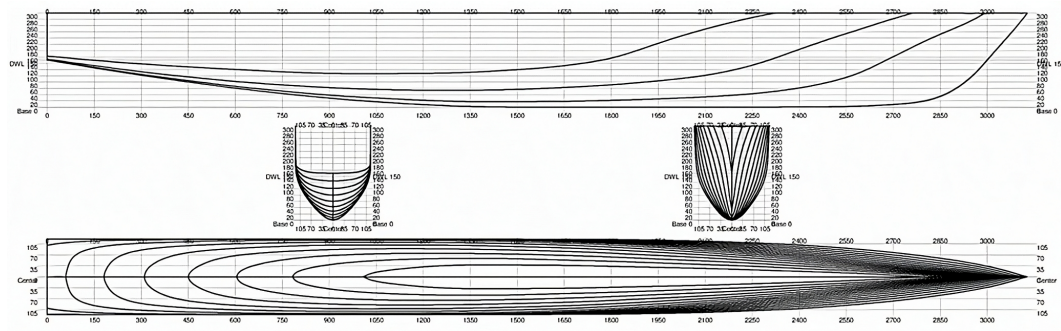


Figure 2: DELFT 372 Catamaran linesplan [39]

Table 1 shows the main dimension of the DELFT 372 catamaran hull model that were used by Veer [39].

Table 1: Main dimension of DELFT 372 catamaran [39]

Main Particulars	Symbol	Value	Unit
Length overall	L_{OA}	3.11	m
Length between perpendicular	L	3.00	m
Beam overall	B	0.94	m
Beam demihull	b	0.24	m
Draught	T	0.15	m
Displacement	Δ	87.07	Kg
Roll radius of gyration	K_{XX}	0.389	m
Pitch radius of gyration	K_{YY}	0.810	m
Yaw radius of gyration	K_{ZZ}	0.930	m
Block coefficient	C_b	0.206	

2.2 DELFT 372 Hydrostatic Verification

Table 2 shows the comparison of hydrostatic properties between the reference values [39] and those computed from the Rhino 6 software of DELFT 372 hull.

Table 2: DELFT 372 symmetry verification

Item	Symbol	DELFT 372 symmetry [39]	DELFT 372 symmetry (Rhino 6 software)	unit	% Diff.
Length (Overall)	L _{OA}	3.11	3.11	m	0
Length between perpendicular	L _{BP}	3.00	3.00	m	0
Beam (Overall)	B	0.94	0.94	m	0
Beam (demihull)	b	0.24	0.24	m	0
Draught	T	0.15	0.15	m	0
Displacement	Δ	87.07	83.41	Kg	4.20
Block coefficient	C _b	0.206	0.197		4.37

The percentage differences in displacement, Δ and block coefficient, C_b for the modelled hull are 4.20% and 4.37%, respectively and are considered acceptable for the purposes of this research. These minor discrepancies are likely due to slight surface inconsistencies introduced during the modelling process.

2.3 DELFT 372 Validation

Seakeeping behavior of the DELFT 372 hull model developed in this study was validated against experiment results by Veer [39]. The validation was performed by comparing the heave and pitch RAO values at a wave amplitude of 0.0179 m and a Froude number of 0.6 under sea state 1 conditions, as presented in Table 3. Seakeeping analysis for DELFT 372 were conducted by using Ansys AQWA at Fr = 0.6 because it represents a realistic high-speed operating condition and ensures comparability with benchmark studies. The differences in heave and pitch RAO values were found to be 4.67% and 8.58% respectively, which demonstrating good agreement with the benchmark data and confirming the model's reliability for subsequent seakeeping analysis. The percentage of difference between 5-10% is considered acceptable for numerical simulation [40]. The slight overestimation of RAO values may be attributed to factors such as the omission of viscous effects in the numerical simulations. As noted by Pols et al. [41], excluding viscous forces in seakeeping analysis can lead to amplified motion responses, resulting in higher RAO values compared to experimental data where such effects are inherently included.

Table 3: Heave validation at sea state 1

Froude number, Fr	Wave Amplitude, A (m)	Period, T (s)	λ (m)	λ/Lpp	Heave RAO (m/m) [39]	Heave RAO (m/m)	Heave % diff	Pitch RAO (°/m), [39]	Pitch RAO (°/m)	Pitch % diff
0.60	0.0179	1.754	4.803	1.601	2.80	2.93	4.67	86.5	93.9	8.58

2.4 DELFT 372 Configurations

Figure 3 shows the OF-Xbow model which was generated by slicing the original DELFT 372 symmetry hull and combining Xbow shape resulting in an asymmetrical configuration. This modification was implemented to leverage the advantages offered by outside flat catamarans which have been shown to improve overall seakeeping performance compared to the original symmetrical hull design [35]. In addition, according to Yehia *et al.*, [36], the Xbow is specifically designed to improve seakeeping capability in rough sea states by minimizing vertical accelerations and wave impacts. However, it can be seen that the

displacement at the same draft has been reduced to 50.46 kg from 83.41 kg. In order to maintain the displacement, the demihull breadth has been increased to 0.2 m which yields 84.11 kg with difference of 0.84 % as compared to the original DELFT 372 symmetry hull as shown in Figure 4. The hydrostatic data for the modified hull is shown in Table 4.

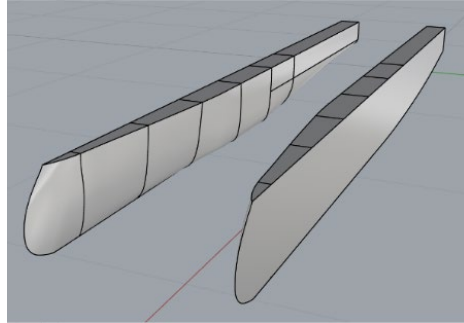


Figure 3: OF-Xbow

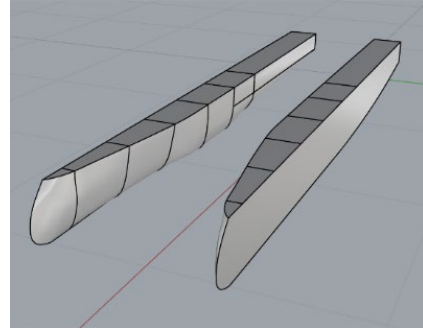


Figure 4: OF-Xbow, b= 0.20 m

Table 4: DELFT 372 modified hull hydrostatic particulars

Item	Symbol	OF-Xbow	OF-Xbow, b =0.2 m	unit
Length (Overall)	L _{OA}	3.11	3.11	m
Length between perpendicular	L _{BP}	3.00	3.00	m
Beam (Overall)	B	0.70	0.86	m
Beam (demihull)	b	0.12	0.20	m
Draught	T	0.15	0.15	m
Displacement	Δ	50.46	84.11	Kg
Block coefficient	C _b	0.15	0.203	

2.5 Heave and Pitch RAO equations

The equation of motion of the ship in the CFD software can be expressed as equation (1):

$$\{m + m_a\}\ddot{X}(t) + c\dot{X}(t) + KX(t) = F(t) \quad (1)$$

where m represents the structural mass matrix, m_a is the fluid added mass matrix at infinite frequency, c denotes the damping matrix incorporating linear radiation damping effects, K is the total stiffness matrix, and $F(t)$ represents the external forces acting on the ship. The Response Amplitude Operator (RAO) is a transfer function that characterizes the motion response of the module and as a function of wave frequency. According to Bosma [42], RAOs are typically expressed in a non-dimensional form relative to wave height and serve as a valuable tool for identifying the frequencies at which maximum power can theoretically be extracted. The RAO can be formulated as shown in equation (2), equation (3), and equation (4).

$$RAO = \frac{F_e^\omega}{K + j\omega C(\omega) - \omega^2(M + Ma(\omega))} \quad (2)$$

$$RAO_{heave} = \frac{\zeta}{A} \quad (\text{m/m}) \quad (3)$$

$$RAO_{pitch} = \frac{\theta}{kA} \quad (\text{rad} \cdot \text{m/m}) \quad (4)$$

where, F_e^ω is the excitation wave force (both incident and diffracting forces). K is the hydrostatic stiffness. M is the mass of the structure. $Ma(\omega)$ is the added mass. $C(\omega)$ is the radiation damping and ω is the wave frequency ω , ζ is heave amplitude and θ is pitch amplitude of the vessel, k is wave number while A is the wave amplitude.

2.6 Grid Independence Test (GIT)

The Grid Independence Test (GIT) was conducted using meshing settings in Ansys AQWA to determine the optimal mesh size for simulation and to minimize numerical errors. Table 5 presents the GIT results for the symmetric hull while Figure 5 illustrates the corresponding GIT curve for the DELFT 372 symmetric model. The results indicate that the heave and pitch RAO values begin to converge at a total mesh element count of approximately 13,000.

Table 5: GIT for DELFT 372 symmetry

Item (no. of element)	Global size (m)	Local size (m)	Total element
Coarse	0.16316	0.16316	12,660
Medium	0.12	0.09	13,178
Fine	0.1	0.07	13,524

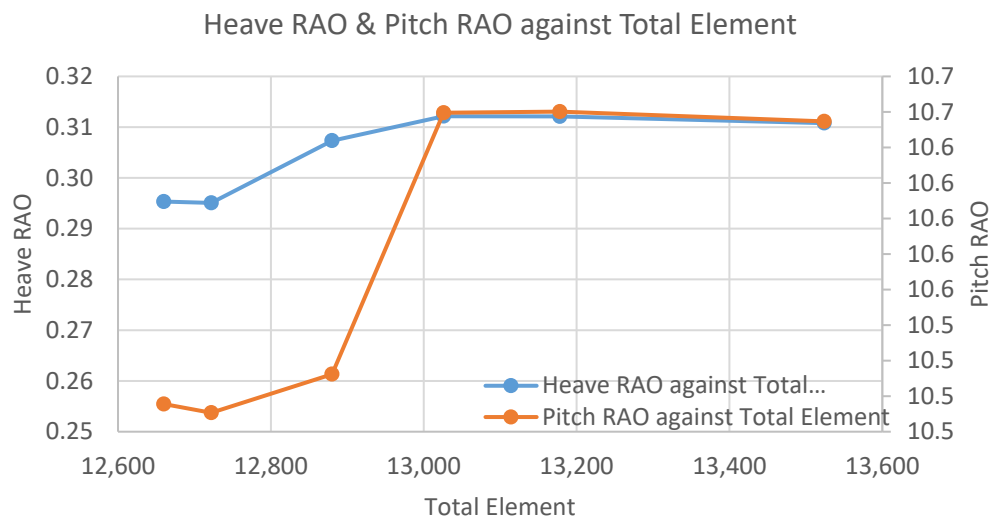


Figure 5: GIT curve for DELFT 372 symmetry

To reduce computational time while maintaining accuracy, the selected mesh settings use a global size of 0.12 m and a local size of 0.09 m, resulting in a total of 13,178 elements. At this mesh density, the heave and pitch RAO values begin to converge and demonstrate consistent results.

2.7 Seakeeping Analysis Domain

The computational domain, illustrated in Figure 6, was generated with dimensions of $x = 10 L_{OA}$ (31.1 m) in length, $y = 4.5 L_{OA}$ (14 m) in width, and $z = 50$ m in depth, based on the sea conditions at Pengerang, Kota Tinggi. The origin of the coordinate system was located at the ship's centroid and aligned with the calm water surface. The longitudinal and

transverse positions of the model coincided with the aft end and centerline of the vessel, respectively, with the positive x-axis directed toward the bow, the y-axis toward the port side, and the z-axis oriented vertically upwards. The waves originated from two orthogonal directions with zero phase difference. As illustrated in Figure 7, the wave heading angle was set at 180° .

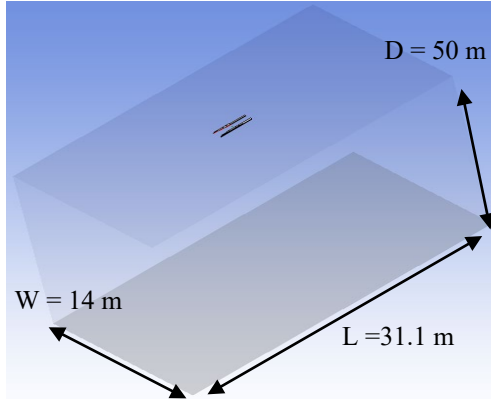


Figure 6: Domain of DELFT 372 on Ansys AQWA pre-processor phase

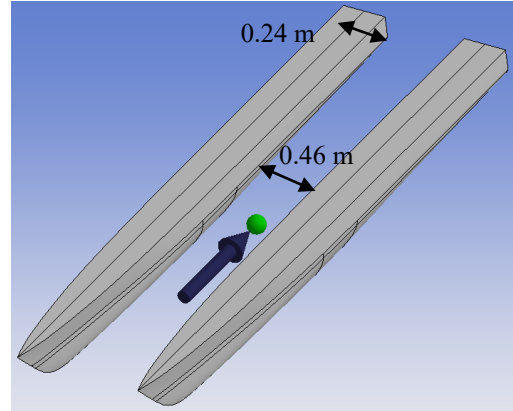


Figure 7: Wave heading angle of DELFT 372 symmetry

The wave heading of 180° was also applied to the OF-Xbow and OF-Xbow, $b=0.2$ m, as illustrated in Figures 8 and 9. Only one wave direction was considered in this seakeeping analysis. Table 6 shows the seakeeping matrix applied in this research where the period, T and wavelength, λ range are chosen under sea state 2 conditions based on [43]. All configurations were analysed at a Froude number of 0.6, with a wave amplitude, A of 0.25 m, under sea state 2 conditions using the specified computational domain setup.

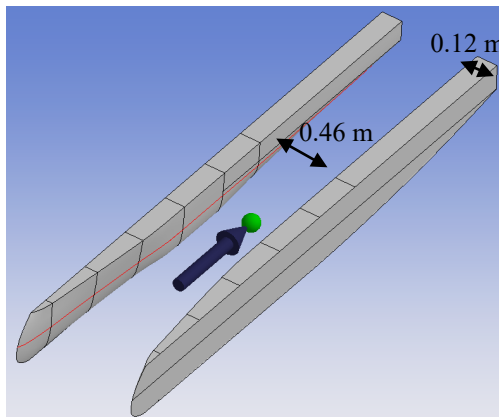


Figure 8: Wave heading angle of DELFT 372 OF-Xbow

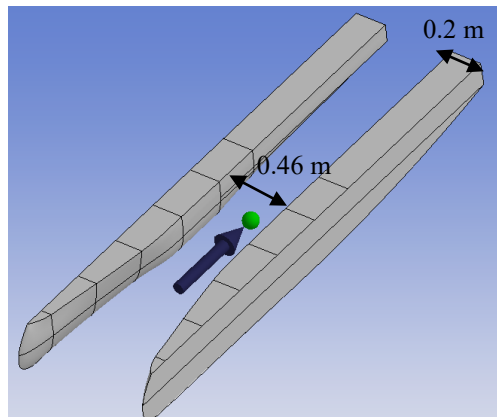


Figure 9: Wave heading angle of DELFT 372 OF-Xbow, $b=0.2$ m

Table 6: Seakeeping test matrix for both modified hull form at sea state 2

Froude number, Fr	Wave Amplitude, A (m)	Period, T (s)	λ (m)	λ/L_{pp}
0.60	0.25	2.372	8.79	2.93
		2.693	11.32	3.77
		2.979	13.86	4.62
		3.241	16.40	5.47
		3.482	18.93	6.31

3.708	21.47	7.16
3.921	24.01	8.00
4.123	26.54	8.85
4.316	29.08	9.69

3.0 RESULTS AND DISCUSSION

Seakeeping simulations were conducted based on potential flow diffraction theory for a vessel operating in head regular waves. The selected Froude number was 0.6, with wave characteristics defined as described in the previous section. The simulations were performed under steady-state conditions to capture all relevant motions, including heave and pitch. The primary objective of this study is to compute the ship's RAO values using numerical methods implemented in Ansys AQWA. The vessel's response to waves with a 0.25 m amplitude was analysed, and the predicted heave and pitch RAO values obtained from Ansys AQWA are presented in the following graphical results.

3.1 DELFT 372 symmetry

Before proceeding with seakeeping analysis of the modified hull, it is vital to analyze the basis hull and set it as reference value. Table 7 shows the results of DELFT 372 hull form simulated from Ansys AQWA. Heave and pitch RAO were calculated from the result obtained by using equation (3) and equation (4).

Table 7: Seakeeping result for DELFT symmetry at sea state 2

Froude number, Fr	Wave Amplitude, A (m)	Period, T (s)	λ (m)	λ/L_{pp}	Heave Amplitude (m)	Pitch Amplitude (rad)	Heave RAO	Pitch RAO
0.60	0.25	2.372	8.79	2.93	0.2775	0.2624	1.11	1.47
		2.693	11.32	3.77	0.2375	0.2016	0.95	1.45
		2.979	13.86	4.62	0.2125	0.1740	0.85	1.54
		3.241	16.40	5.47	0.2000	0.1595	0.80	1.67
		3.482	18.93	6.31	0.1950	0.1518	0.78	1.83
		3.708	21.47	7.16	0.1925	0.1477	0.77	2.02
		3.921	24.01	8.00	0.1950	0.1457	0.78	2.23
		4.123	26.54	8.85	0.1975	0.1447	0.79	2.45
		4.316	29.08	9.69	0.2000	0.1443	0.80	2.67

The result shows that the heave RAO values exhibit a decreasing trend as the λ/L_{pp} ratio increases. The minimum heave and pitch RAO values for this hull configuration are 0.77 m/m and 1.45 rad/m, respectively, occurring at λ/L_{pp} ratios of 7.16 and 3.77. Conversely, the peak heave and pitch RAO values are 1.11 m/m and 2.67 rad/m respectively at a λ/L_{pp} of 2.93 and 9.69. The tabulated results are plotted to generate the heave and pitch RAO curves, as illustrated in Figure 10. Heave RAO display a declining trend while pitch RAO display a inclining trend. The reduction in heave amplitude with increasing λ/L_{pp} leads to a corresponding decrease in heave RAO values. This behaviour is attributed to the diminishing wave excitation forces at higher λ/L_{pp} ratios. As λ/L_{pp} increases, the wavelength becomes considerably longer relative to the vessel length, allowing the vessel to span a greater portion of the wave. This results in a more uniform distribution of wave-induced forces along the hull, thereby reducing vertical motions. In contrast, at lower λ/L_{pp} values, shorter waves relative to the vessel length induce larger vertical displacements, leading to higher heave RAO values. A different trend is observed for pitch motions, which increase as λ/L_{pp} increases. This due to longer waves reduce the wave slope and because

alternating buoyancy at bow and stern is strongest when λ is comparable to ship length, leading to large pitching moments.

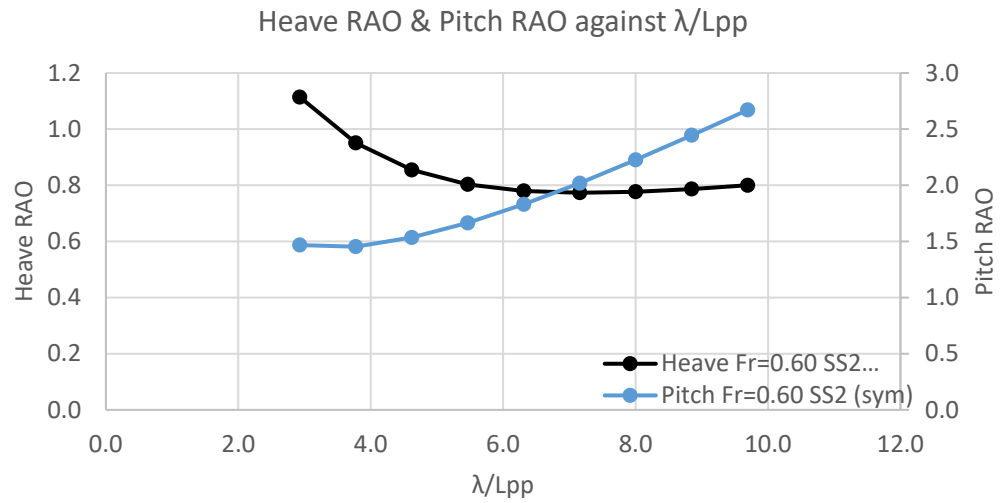


Figure 10: Heave & Pitch RAO against λ/L_{pp} (DELFT 372 symmetry)

Figure 11 shows the simulation that has been performed to determine the heave and pitch RAO value. The heave and pitch RAO value are obtained and then tabulated as in Table 8 and the seakeeping curve is plotted. Seakeeping analysis were analyzed at wave amplitude of 0.25 m, at Fr of 0.6 in the sea state 2 condition as referred to sea state at Pengerang Kota Tinggi.

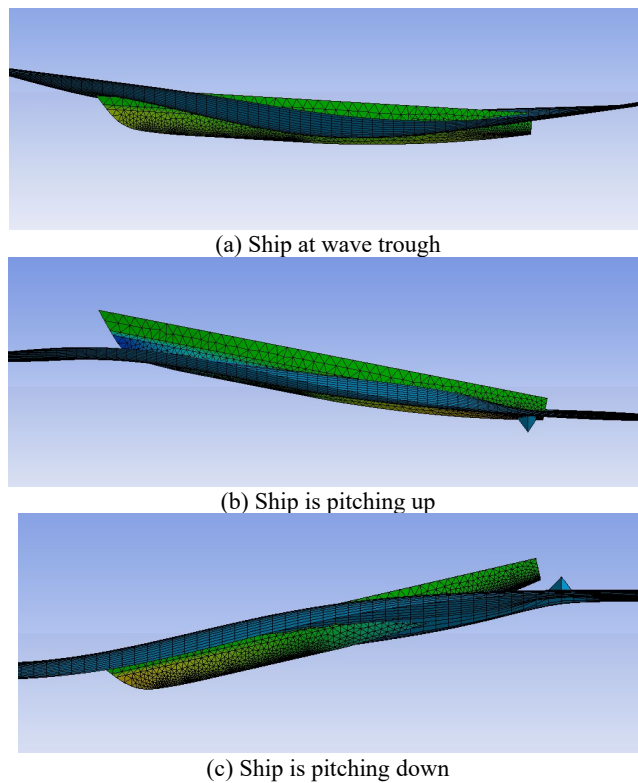


Figure 11: Original DELFT 372 symmetry hull simulation

3.2 DELFT 372 OF-Xbow

Table 8 displays the seakeeping analysis results for the DELFT 372 OF-Xbow that has been analysed under the sea state 2 condition using Ansys AQWA.

Table 8: Seakeeping result for DELFT OF-Xbow at sea state 2

Froude number, Fr	Wave Amplitude, A (m)	Period, T (s)	λ (m)	λ/L_{pp}	Heave Amplitude (m)	Pitch Amplitude (rad)	Heave RAO	Pitch RAO
0.60	0.25	2.372	8.79	2.93	0.2650	0.2186	1.06	1.22
		2.693	11.32	3.77	0.2425	0.1706	0.97	1.23
		2.979	13.86	4.62	0.2325	0.1379	0.93	1.22
		3.241	16.40	5.47	0.2300	0.1129	0.92	1.18
		3.482	18.93	6.31	0.2300	0.0940	0.92	1.13
		3.708	21.47	7.16	0.2350	0.0792	0.94	1.08
		3.921	24.01	8.00	0.2375	0.0678	0.95	1.04
		4.123	26.54	8.85	0.2400	0.0588	0.96	0.99
		4.316	29.08	9.69	0.2425	0.0517	0.97	0.96

The table presents the seakeeping analysis results focusing on the heave and pitch RAO values. It is observed that, as the λ/L_{pp} ratio increases, both heave and pitch RAO values exhibit a decreasing trend. For this specific hull configuration, the minimum heave and pitch RAO values are 0.92 and 0.96 at λ/L_{pp} ratios of 5.47 and 9.69, respectively. In contrast, the maximum values reach 1.06 and 1.23 at a λ/L_{pp} ratio of 2.93 and 3.77 respectively. The tabulated data were used to generate the heave and pitch RAO curves, as shown in Figure 12. As λ/L_{pp} increases, the heave amplitude decreases resulting in a reduction of the heave RAO. This reduction is attributed to a decrease in wave excitation forces. When λ/L_{pp} becomes larger, the waves grow significantly longer relative to the vessel length, causing the ship to span a greater portion of the wave. As a result, wave-induced forces are more evenly distributed along the hull, thereby reducing vertical motion. In contrast, at low λ/L_{pp} ratios, shorter waves induce greater vertical movement leading to higher heave RAO values. A slight increase in the heave RAO is observed within the λ/L_{pp} range of 6.31 to 9.69, which may be attributed to hull modifications from the original design to the OF-Xbow, introducing wave interactions between the hulls at higher λ/L_{pp} ratios.

A similar pattern whichs observed whichn the pitch motion whichh also decreases as the λ/L_{pp} ratio increases. This behaviour is attributed to the reduction in wave-induced moments acting on the vessel. At low λ/L_{pp} ratios, the vessel undergoes alternating bow and stern submersion, resulting in significant pitch motion. However, as λ/L_{pp} increases, the vessel spans multiple wave crests and troughs more uniformly thereby reducing its tendency to pitch.

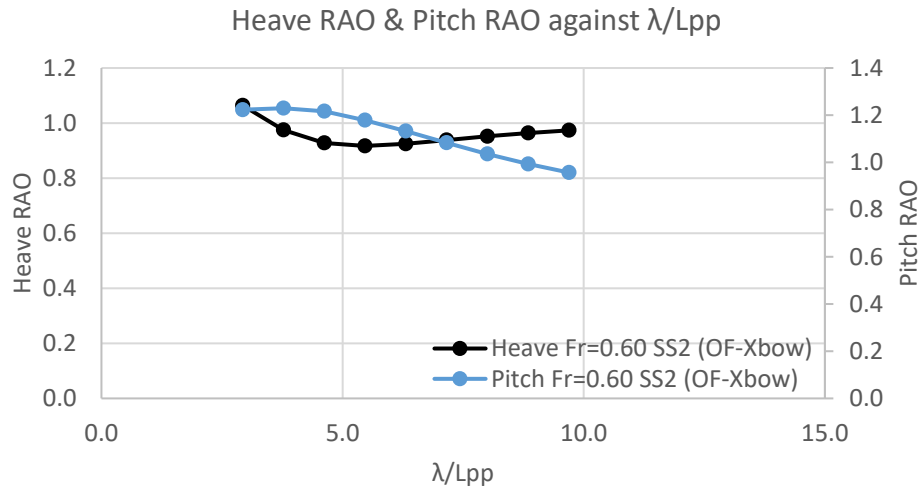


Figure 12: Heave & Pitch RAO against λ/L_{pp} (DELFT 372 OF-Xbow)

The Figure 13 depicts the simulation performed in Ansys AQWA to evaluate the heave and pitch RAO values, which were extracted and the seakeeping curve is plotted.

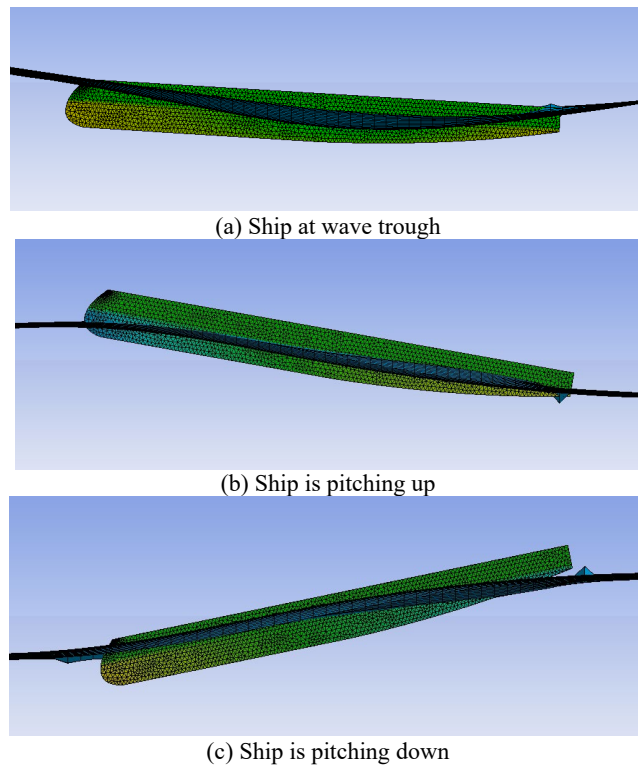


Figure 13: DELFT 372 OF-Xbow simulation

3.3 DELFT 372 OF-Xbow with $b = 0.2$ m

Table 9 displays the seakeeping analysis results for the DELFT 372 OF-Xbow, $b=0.20$ m that has been analysed under the sea state 2 condition using Ansys AQWA.

Table 9: Seakeeping result for OF-Xbow, b=0.2 m at sea state 2

Froude number, Fr	Wave Amplitude, A (m)	Period, T (s)	λ (m)	λ/Lpp	Heave Amplitude (m)	Pitch Amplitude (rad)	Heave RAO	Pitch RAO
0.60	0.25	2.372	8.79	2.93	0.2625	0.2387	1.05	1.34
		2.693	11.32	3.77	0.2325	0.1876	0.93	1.35
		2.979	13.86	4.62	0.2150	0.1626	0.86	1.43
		3.241	16.40	5.47	0.2075	0.1465	0.83	1.53
		3.482	18.93	6.31	0.2075	0.1357	0.83	1.64
		3.708	21.47	7.16	0.2100	0.1280	0.84	1.75
		3.921	24.01	8.00	0.2150	0.1220	0.86	1.87
		4.123	26.54	8.85	0.2200	0.1172	0.88	1.98
		4.316	29.08	9.69	0.2250	0.1129	0.90	2.09

The table presents the seakeeping analysis results focusing on the heave and pitch RAO values. It is observed that, as the λ/Lpp ratio increases, heave RAO values exhibit a decreasing trend and pitch RAO values exhibit an increasing trend. For this specific hull configuration, the minimum heave and pitch RAO values are 0.83 and 1.34 at λ/Lpp ratios of 6.31 and 2.93, respectively. In contrast, the maximum heave and pitch RAO values reach 1.05 and 2.09 at λ/Lpp ratio of 2.93 and 9.69 respectively. The tabulated data were used to generate the heave and pitch RAO curves, as shown in Figure 14. As λ/Lpp increases, the heave amplitude decreases resulting in a reduction of the heave RAO. This reduction is attributed to a decrease in wave excitation forces. When λ/Lpp becomes larger, the waves grow significantly longer relative to the vessel length, causing the ship to span a greater portion of the wave. As a result, wave-induced forces are more evenly distributed along the hull, thereby reducing vertical motion. In contrast, at low λ/Lpp ratios, shorter waves induce greater vertical movement leading to higher heave RAO values. A slight increase in the heave RAO is observed within the λ/Lpp range of 7.16 to 9.69, which may be attributed to hull modifications from the original design to the OF-Xbow, b=0.20m, introducing wave interactions between the hulls at higher λ/Lpp ratios. A different trend is observed for pitch motion, which increases as λ/Lpp grows. This behavior arises because longer waves reduce the wave slope, while the alternating buoyancy between the bow and stern is most pronounced when the wavelength is comparable to the ship length, resulting in larger pitching moments.

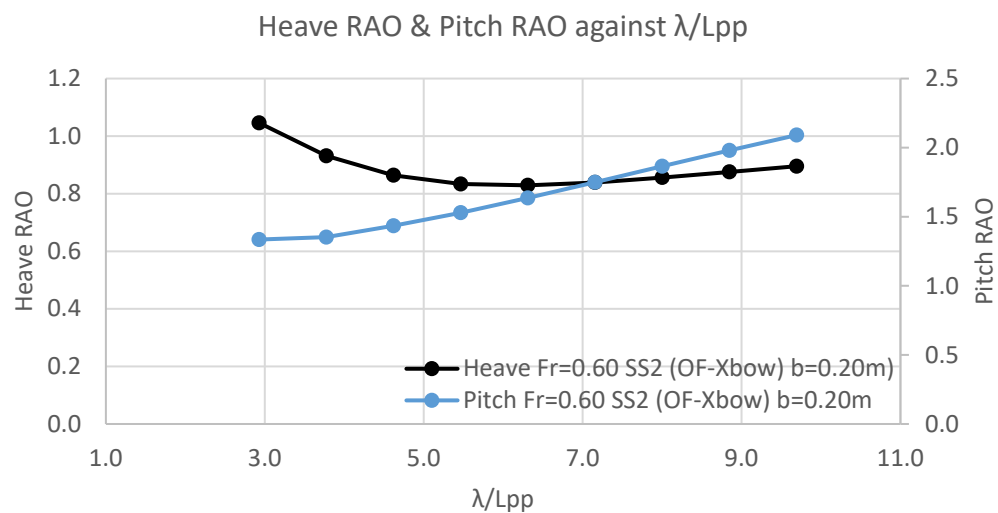


Figure 14: Heave & Pitch RAO against λ/Lpp (DELFT 372 OF-Xbow, b=0.2 m)

The Figure 15 depicts the simulation performed in Ansys AQWA to evaluate the heave and pitch RAO values, which were extracted and the seakeeping curve is plotted.

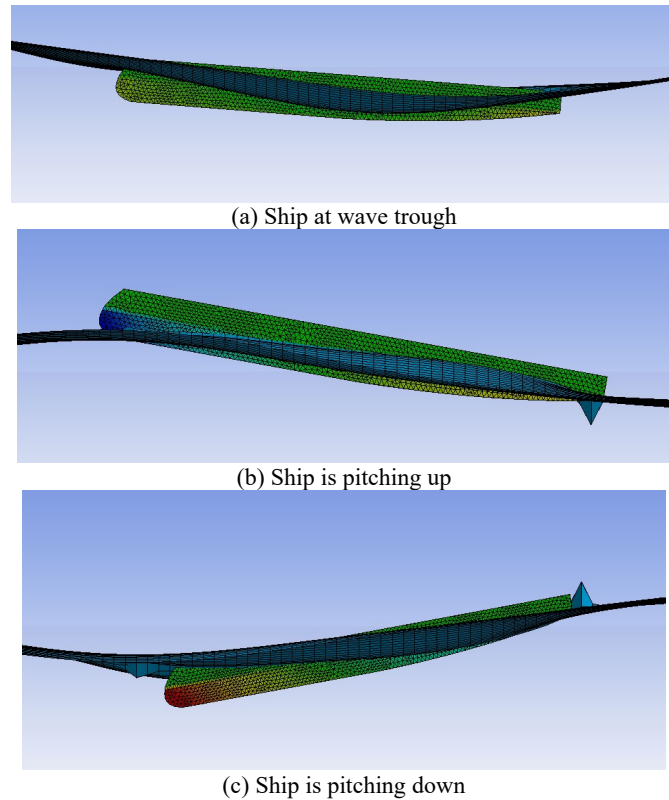


Figure 15: DELFT 372 OF-Xbow, $b=0.2$ m simulation

3.4 Comparison for all DELFT 372 configuration

After gaining all results, both heave and pitch RAO were plotted and the trend curve were obtained. The heave and pitch RAO were compared and plotted in the same curve as shown in Figure 16 and 17. Figure 16 shows the heave RAO comparison for the symmetry (original), OF-Xbow and OF-Xbow, $b=0.2$ m. In general, the heave RAO response is ranging from 0.77 to 1.11 indicating the heave motion is not significant for this hull. At the lowest λ/L_{pp} of 2.93, the heave RAO improves slightly by 4.50% for the OF-Xbow and 6.11% for the OF-Xbow, $b=0.20$ m relative to the symmetric hull, indicating that both modified hulls exhibit reduced heave motion under these conditions. However, as λ/L_{pp} increases from 3.77 to 9.69, the heave motion of the modified DELFT 372 hulls increases 21.7% for the OF-Xbow and 11.9% for the OF-Xbow, $b=0.20$ m at λ/L_{pp} of 9.69.

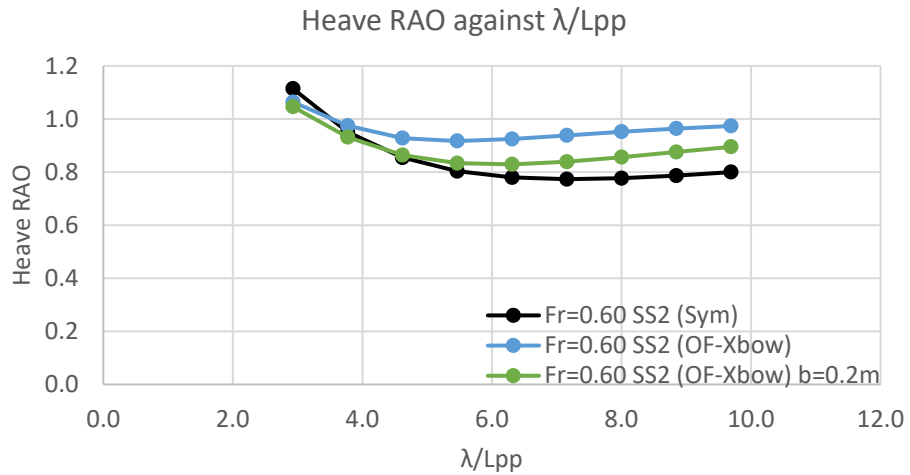


Figure 16: Heave RAO against λ/L_{pp} curve comparison

Meanwhile, Figure 17 presents the pitch RAO comparison among the studied hull. It can be observed that the OF-Xbow consistently exhibits the lowest pitch RAO values indicating superior pitch motion reduction compared to both the symmetry and OF-Xbow, $b=0.2m$ hulls. Specifically, at λ/L_{pp} of 9.69, the OF-Xbow and OF-Xbow, $b=0.2m$ achieve pitch RAO values of 0.96 and 2.09 representing improvements of 64.17% and 21.72% respectively over the symmetry hull. Similarly at a lower λ/L_{pp} of 2.93, the OF-Xbow and OF-Xbow, $b=0.20m$ yield pitch RAO values of 1.22 and 1.34 corresponding to improvements of 16.28% and 9.06% respectively. From these comparisons, it can be concluded that both the OF-Xbow and OF-Xbow, $b=0.20m$ configurations offer overall improvements in pitch motion, though at the cost of increased heave motion under sea state 2 conditions, which is deemed not significant. By maintaining a low pitch RAO motion which helps reduce excessive movement and vibration, the pH sensors that used by the USV and others can operate under optimal conditions. USV become more efficient and reliable when sensors function in such favorable conditions, the data collected during monitoring activities remains stable and more accurate.

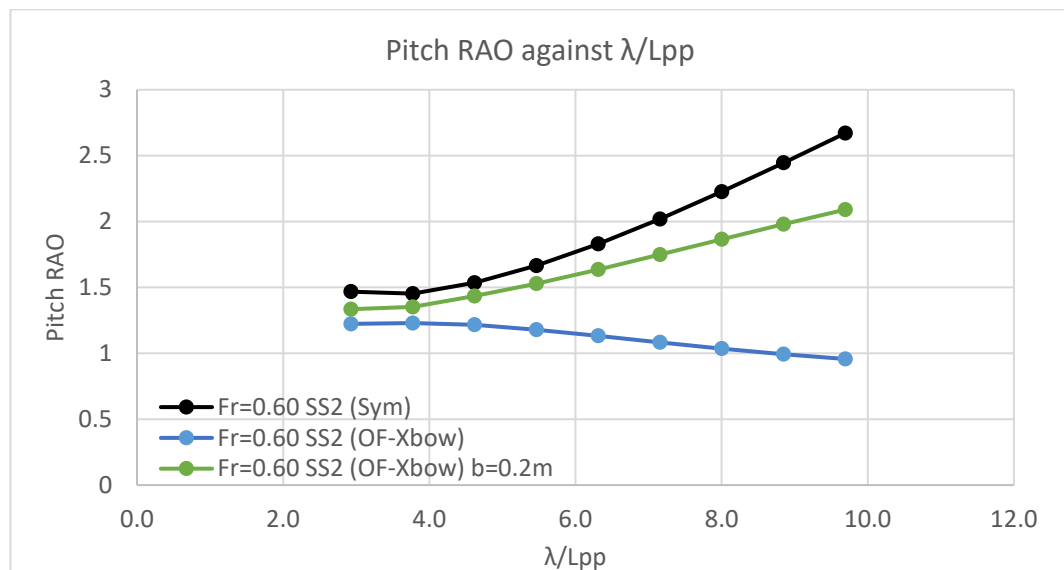


Figure 17: Pitch RAO against λ/L_{pp} curve comparison

4.0 CONCLUSION

In this study, a seakeeping analysis of the DELFT 372 with all hull configurations was conducted and compared under Sea State 2 conditions using Ansys AQWA. Numerical simulations were performed at a Froude number of 0.6, predicting the vessel's heave and pitch RAOs with a wave amplitude of 0.25 m. The Froude number was found to significantly influence the motion response, allowing for an accurate representation of the vessel's seakeeping behavior. The results reveal that the heave and pitch RAO values for the OF-Xbow are 0.97 and 0.96 respectively, while for the OF-Xbow, $b = 0.20$ m, the values are 0.90 and 2.09 at λ/L_{pp} of 9.69. These values were compared to those of the symmetric hull, which exhibited a heave RAO of 0.80 and a pitch RAO of 2.67. The findings demonstrate a substantial reduction in pitch motion, with improvements of 64.17% for the OF-Xbow and 21.72% for the OF-Xbow, $b = 0.20$ m, compared to the symmetric hull at λ/L_{pp} of 9.69. However, at λ/L_{pp} of 9.69, the heave motion increased by 21.72% and 11.91%, respectively for the OF-Xbow and OF-Xbow with $b = 0.20$ m respectively, because the waterplane area and added mass were reduced with narrower demihulls compared to the symmetric hull with larger demihulls. A narrower demihull leads to a weaker restoring buoyancy force, which directly lowers the hydrostatic stiffness and makes the hull oscillate more easily. This study confirms that hull modifications can significantly improve pitch motion performance, albeit at the cost of increased heave motion. The primary objective of this research has been achieved, as the OF-Xbow and OF-Xbow, $b = 0.20$ m exhibit improved performance compared to the symmetric hull configuration. Despite substantial improvements in pitch response, the USV may still face operational limitations due to increased heave motion, which could compromise its ability to perform monitoring tasks effectively. The maximum λ/L_{pp} ratio for the safe operation of this USV is identified as 9.69. Beyond this value, further increases in λ/L_{pp} may exacerbate the heave response due to the rising heave RAO, thereby restricting the USV's operability in conditions exceeding Sea State 2, primarily to ensure equipment safety. For safe operations, the USV should be limited to Sea State 2 conditions, where the maximum allowable wave amplitude is 0.25 m. To further enhance the vessel's operability, future research should explore the integration of novel hull designs or passive/active devices aimed at reducing heave motion while maintaining low pitch amplitudes. One potential solution to mitigate heave motion is the implementation of fin stabilizers on the USV hull.

ACKNOWLEDGEMENT

This research was supported by the Universiti Teknologi Malaysia under the Encouragement Grant (UTMER) with Project Reference No: PY/2023/01181 and its cost centre Q.J130000.3824.31J53 and UTM COE/RG Reseach Grant with Project Reference No: PJ/2025/00039 and its cost centre Q.J130000.5024.10G56. The authors would like to express their gratitude to the Universiti Teknologi Malaysia for their financial support.

REFERENCES

1. Khan, Muhammad Imran, Koushik Mukherjee, Rizwan Shoukat, and Huang Dong. "A review on pH sensitive materials for sensors and detection methods." *Microsystem Technologies* 23, no. 10 (2017): 4391-4404.
2. Migeotte, Gunther. "Design and optimization of hydrofoil-assisted catamarans." PhD diss., Stellenbosch: Stellenbosch University, 2002.
3. Rollings, Sarah E. "Seakeeping analysis of small displacement high-speed vessels." PhD diss., Monterey, CA; Naval Postgraduate School, 2003.

4. Hadler, J. B., C. M. Lee, J. T. Birmingham, and H. D. Jones. "Ocean Catamaran Seakeeping Design, Based on The Experiments of USNS HAYES." (1974).
5. Kogan, E. M. "To hydrodinamical theory of oscillations of catamaran in liquid of finite depth." *Proceedings of Nikolaev Shipbuilding Institute of adm. SO Makarov. Ships theory (Труды НКИ. Теория корабля)* 35 (1970): 33-39.
6. Kogan, E. M. "To the calculation of main part of disturbing forces for oscillating catamaran in liquid of finite depth." *Proceedings of Nikolaev Shipbuilding Institute of adm. SO Makarov. Ships theory (Труды НКИ. Теория корабля)* 44 (1971): 42-45.
7. Grigoropoulos, Gregory J., and T. A. Loukakis. "Seakeeping performance assessment of planing hulls." *WIT Transactions on The Built Environment* 12 (2025).
8. Aimin, D. E. N. G. "Study on Prediction Methodology of Seakeeping for WPC." *Chinese Journal of Ship Research* 1, no. 01 (2006): 77-80.
9. Guo, Z. Q., Q. W. Ma, and J. L. Yang. "A seakeeping analysis method for a high-speed partial air cushion supported catamaran (PACSCAT)." *Ocean Engineering* 110 (2015): 357-376. <https://doi.org/10.1016/j.oceaneng.2015.10.031>.
10. Fang, Chih-Chung, and Hoi-Sang Chan. "Investigation of seakeeping characteristics of high-speed catamarans in waves." *Journal of Marine Science and Technology* 12, no. 1 (2004): 2. <https://doi.org/10.51400/2709-6998.2215>.
11. French, Benjamin, Giles Thomas, Michael Davis, and Damien Holloway. "A high Froude number time-domain strip theory for ship motion predictions in irregular waves." In *18th Australasian fluid mechanics conference*, pp. 1-4. 2012.
12. Han, Soonhung, Yeon-Seung Lee, and Young Bok Choi. "Hydrodynamic hull form optimization using parametric models." *Journal of marine science and technology* 17 (2012): 1-17. <https://doi.org/10.1007/s00773-011-0148-8>.
13. Thomas, Giles, Stefan Winkler, Michael Davis, Damien Holloway, Shinsuke Matsubara, Jason Lavroff, and Ben French. "Slam events of high-speed catamarans in irregular waves." *Journal of marine science and technology* 16, no. 1 (2011): 8-21. <https://doi.org/10.1007/s00773-010-0105-y>.
14. Castiglione, Teresa, Frederick Stern, Sergio Bova, and Manivannan Kandasamy. "Numerical investigation of the seakeeping behavior of a catamaran advancing in regular head waves." *Ocean Engineering* 38, no. 16 (2011): 1806-1822. <https://doi.org/10.1016/j.oceaneng.2011.09.003>.
15. Soars, A. J. "The hydrodynamic development of large wave piercing catamarans." (1993).
16. Broglia, Riccardo, Boris Jacob, Stefano Zaghi, Frederick Stern, and Angelo Olivieri. "Experimental investigation of interference effects for high-speed catamarans." *Ocean Engineering* 76 (2014): 75-85. <https://doi.org/10.1016/j.oceaneng.2013.12.003>.
17. Vakilabadi, Karim Akbari, Mohammad Reza Khedmati, and Mohammad Saeed Seif. "Experimental study on heave and pitch motion characteristics of a wave-piercing trimaran." *Transactions of FAMENA* 38, no. 3 (2014): 13-26. <https://doi.org/129609>.
18. Begovic, Ermina, C. Bertorello, and Silvia Pennino. "Experimental seakeeping assessment of a warped planing hull model series." *Ocean Engineering* 83 (2014): 1-15. <https://doi.org/10.1016/j.oceaneng.2014.03.012>.
19. Bouscasse, Benjamin, Riccardo Broglia, and Frederick Stern. "Experimental investigation of a fast catamaran in head waves." *Ocean engineering* 72 (2013): 318-330. <https://doi.org/10.1016/j.oceaneng.2013.07.012>.
20. Kim, Dong Jin, Sun Young Kim, Young Jun You, Key Pyo Rhee, Seong Hwan Kim, and Yeon Gyu Kim. "Design of high-speed planing hulls for the improvement of resistance and seakeeping performance." *International Journal of Naval Architecture and Ocean Engineering* 5, no. 1 (2013): 161-177. <https://doi.org/10.3744/JNAOE.2013.5.1.161>.
21. Diez, Matteo, Riccardo Broglia, Danilo Durante, Emilio F. Campana, and Frederick Stern. "Validation of high-fidelity uncertainty quantification of a high-speed catamaran in irregular waves." In *SNAME International Conference on Fast Sea Transportation*, p. D021S005R017. SNAME, 2015. <https://doi.org/10.5957/FAST-2015-040>.
22. Haase, Max, Konrad Zurcher, Gary Davidson, Jonathan R. Binns, Giles Thomas, and Neil Bose. "Novel CFD-based full-scale resistance prediction for large medium-speed catamarans." *Ocean Engineering* 111 (2016): 198-208. <https://doi.org/10.1016/j.oceaneng.2015.10.018>.
23. Iglesias, A. Souto, R. Zamora, D. Fernández, and C. López Pavón. "Catamaran wave resistance and central wave cuts for CFD validation." In *Maritime Transportation and Exploitation of Ocean and Coastal Resources: Proceedings of the 11th International Congress of the International Maritime Association of the Mediterranean, Lisbon, Portugal*. <http://dx.doi.org/10.1201/9781439833728.ch1>, vol. 8. 2006.
24. Salas, M., R. Luco, P. K. Sahoo, N. Browne, and M. Lopez. "Experimental and CFD resistance calculation of a small fast catamaran." *Proceeding of International Conference on High-Performance Vehicles* 215 (2004).
25. Swidan, Ahmed Abdelwahab Wahby. "Catamaran wetdeck slamming: a numerical and experimental investigation." PhD diss., University Of Tasmania, 2016. <https://doi.org/23240618/40957565>.

26. Ozturk, Deniz, Cihad Delen, Simone Mancini, Mehmet Ozan Serifoglu, and Turgay Hizarci. "Full-scale CFD analysis of double-m craft seakeeping performance in regular head waves." *Journal of Marine Science and Engineering* 9, no. 5 (2021): 504. <https://doi.org/10.3390/jmse9050504>.
27. Nguyen, Van Minh, Thi Loan Mai, Thi Thanh Diep Nguyen, Youngho Park, Bon Guk Koo, Hyun Su Ryu and Hyeon Kyu Yoon. "Numerical Seakeeping Analysis of Container Ship in Regular Waves in Various Wave Directions." *Journal of Transportation Science and Technology*, vol. 29 (2018): 32-38.
28. Fitriadhy, Ahmad, Syarifuddin Dewa, Nurul Aqilah Mansor, Nur Amira Adam, Cheng Yee Ng, and Hooi Siang Kang. "CFD investigation into seakeeping performance of a training ship." *CFD Letters* 13, no. 1 (2021): 19-32. <https://doi.org/10.37934/cfdl.13.1.1932>.
29. Suastika, Ketut, Agung Silaen, Muhammad Hafiz Nurwahyu Aliffrananda, and Yuda Apri Hermawan. "Seakeeping analysis of a hydrofoil supported watercraft (hysuwac): A Case Study." *CFD Letters* 13, no. 5 (2021): 10-27. <https://doi.org/10.37934/cfdl.13.5.1027>.
30. Rocha Filho, Sergio Murilo Daruis, Roger Matsumoto Moreira, Marcio Zamboti Fortes, and Rafael Eitor dos Santos. "CFD Analysis of The Heave and Pitch Motion of Hull Model." *CFD Letters* 14, no. 4 (2022): 14-31. <https://doi.org/10.37934/cfdl.14.4.1431>.
31. Kiryanto, Kiryanto, Ari Wibawa Budi Santosa, Samuel Samuel, and Ahmad Firdhaus. "Sea-keeping analysis of hospital catamarans for handling COVID-19 patients on remote islands with a numerical approach." *International Journal of Advanced and Applied Sciences* 9, no. 8 (2022): 128-135. <https://doi.org/10.21833/ijaas.2022.08.016>.
32. Sahoo, Prasanta K., Nicholas A. Browne, and Marcos Salas. "Experimental and CFD study of wave resistance of high-speed round bilge catamaran hull forms." In *Proceedings of 4th International Euro Conference on High Performance Marine Vehicles, Rome, Italy*. 2004.
33. Cirello, Antonio, Corrado Damiano, Giuseppe Lupo, Antonio Mancuso, and Gabriele Virzi Mariotti. "CFD Study of an Innovative Catamaran with Asymmetrical Hulls." *Advances in Water Resource and Protection* 1, no. 1 (2013): 10.
34. Utama, Ketut Aria Pria, Andi Jamaluddin, and W. D. Aryawan. "Experimental Investigation into The Drag Interference of Symmetrical an Asymmetrical Staggered and Unstaggered Catamarans." *Journal of Ocean Technology* 7, no. 1 (2012).
35. Ikezoe, S., N. Hirata, and Hironori Yasukawa. "Experimental study on seakeeping performance of a catamaran with asymmetric demi-hulls." *Jurnal Teknologi (Sciences & Engineering)* 66, no. 2 (2014). <https://doi.org/10.11113/jt.v66.2494>.
36. Yehia, Waleed, and Hussien Mohamed Hassan. "On the Design of X-bow for Ship Energy Efficiency." (2017). <https://doi.org/320311087>.
37. Basil, Kunjachan T., and C. P. NajdanWaris. "Hull optimisation of fishing trawlers using ulstein x-bow and bilge keel." *International Journal of Engineering Applied Sciences and Technology* 7, no. 2 (2022): 214-220.
38. Chen, Shuling, Beilei Zou, Changzhi Han, and Shiqiang Yan. "Comparative study on added resistance and seakeeping performance of X-bow and wave-piercing monohull in regular head waves." *Journal of Marine Science and Engineering* 10, no. 6 (2022): 813.
39. Van't Veer, A. P. "Experimental results of motions and structural loads on the 372 catamaran model in head and oblique waves." (1998).
40. Qu, Xiaobin, and Yingxue Yao. "Numerical and experimental study of hydrodynamic response for a novel buoyancy-distributed floating foundation based on the potential theory." *Journal of Marine Science and Engineering* 10, no. 2 (2022): 292. <https://doi.org/10.3390/jmse10020292>.
41. Pols, Alana, Eric Gubesch, Nagi Abdussamie, Irene Penesis, and Christopher Chin. "Mooring analysis of a floating OWC wave energy converter." *Journal of Marine Science and Engineering* 9, no. 2 (2021): 228. <https://doi.org/10.3390/jmse9020228>.
42. Bosma, Bret. "On the design, modelling, and testing of ocean wave energy converters." (2013). <http://doi.org/1957/41003>.
43. Muzathik, A. M. "Wave energy potential of peninsular Malaysia." (2010).